

## **Supporting Information**

# **Morphological study of bicontinuous concentric lamellar silica synthesized at atmospheric pressure and its application as an internal micro-reflector in dye-sensitized solar cells**

*Nadiatus Silmi<sup>a,b</sup>, Rafiq Arsyad<sup>a</sup>, Didi Prasetyo Benu<sup>a,b,c</sup>, Fairuz Gianirfan Nugroho<sup>d,e</sup>, Wiji Lestari Khasannah<sup>a</sup>, Muhammad Iqbal<sup>f</sup>, Brian Yuliarto<sup>e,f</sup>, Rino Rakhmata Mukti<sup>a,e,g</sup>, Veinardi Suendo<sup>a,e\*</sup>*

<sup>a</sup> Division of Inorganic and Physical Chemistry, Faculty of Mathematics and Natural Sciences, Institut Teknologi Bandung, Bandung 40132, Indonesia.

<sup>b</sup> Doctoral Program of Chemistry, Faculty of Mathematics and Natural Sciences, Institut Teknologi Bandung, Bandung 40132, Indonesia.

<sup>c</sup> Department of Chemistry, Universitas Timor, Kefamenanu 85613, Indonesia.

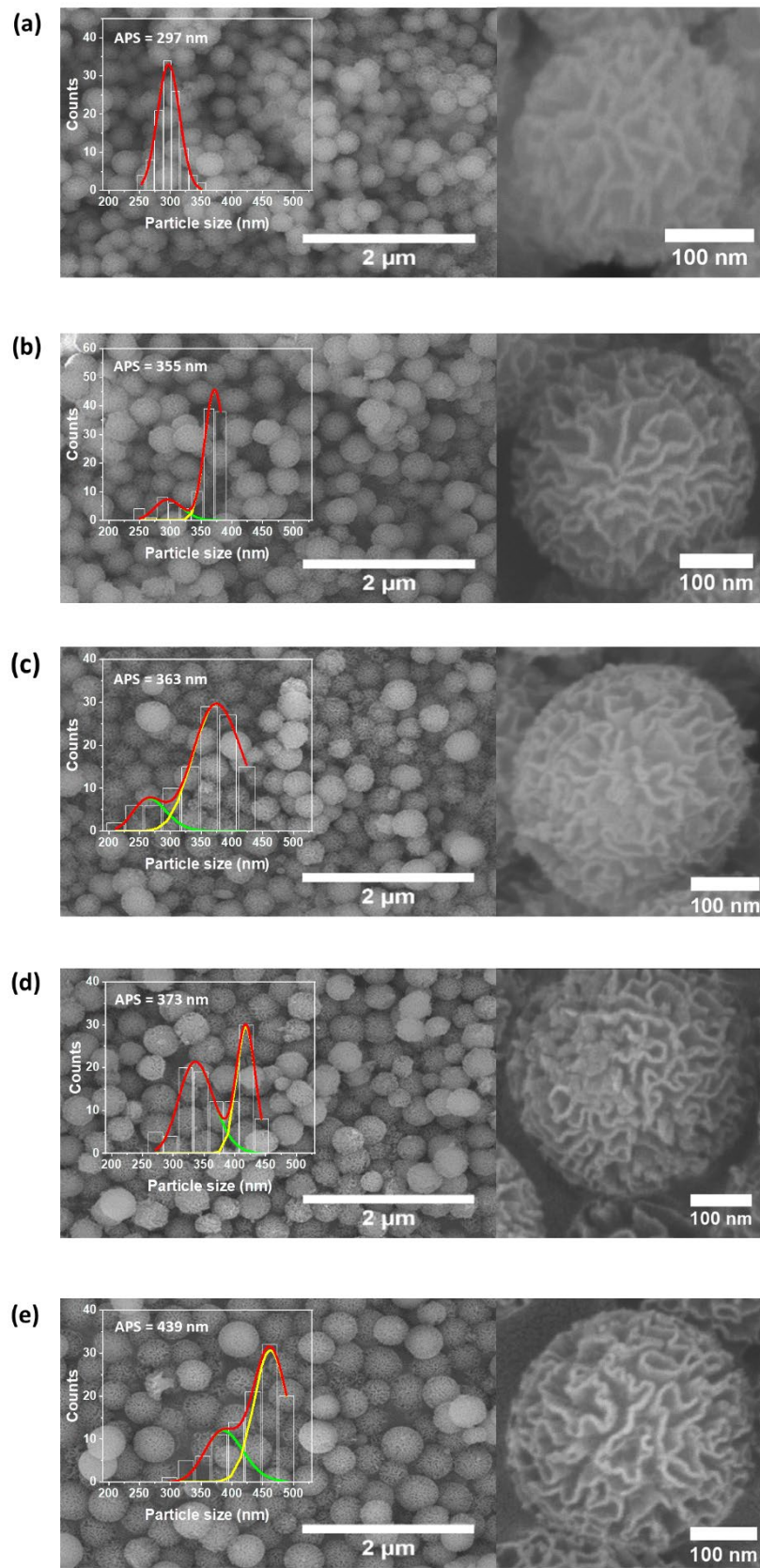
<sup>d</sup> Master's Program in Nanotechnology, Graduate School, Institut Teknologi Bandung, Bandung 40132, Indonesia.

<sup>e</sup> Research Center for Nanosciences and Nanotechnology, Institut Teknologi Bandung, Bandung 40132, Indonesia.

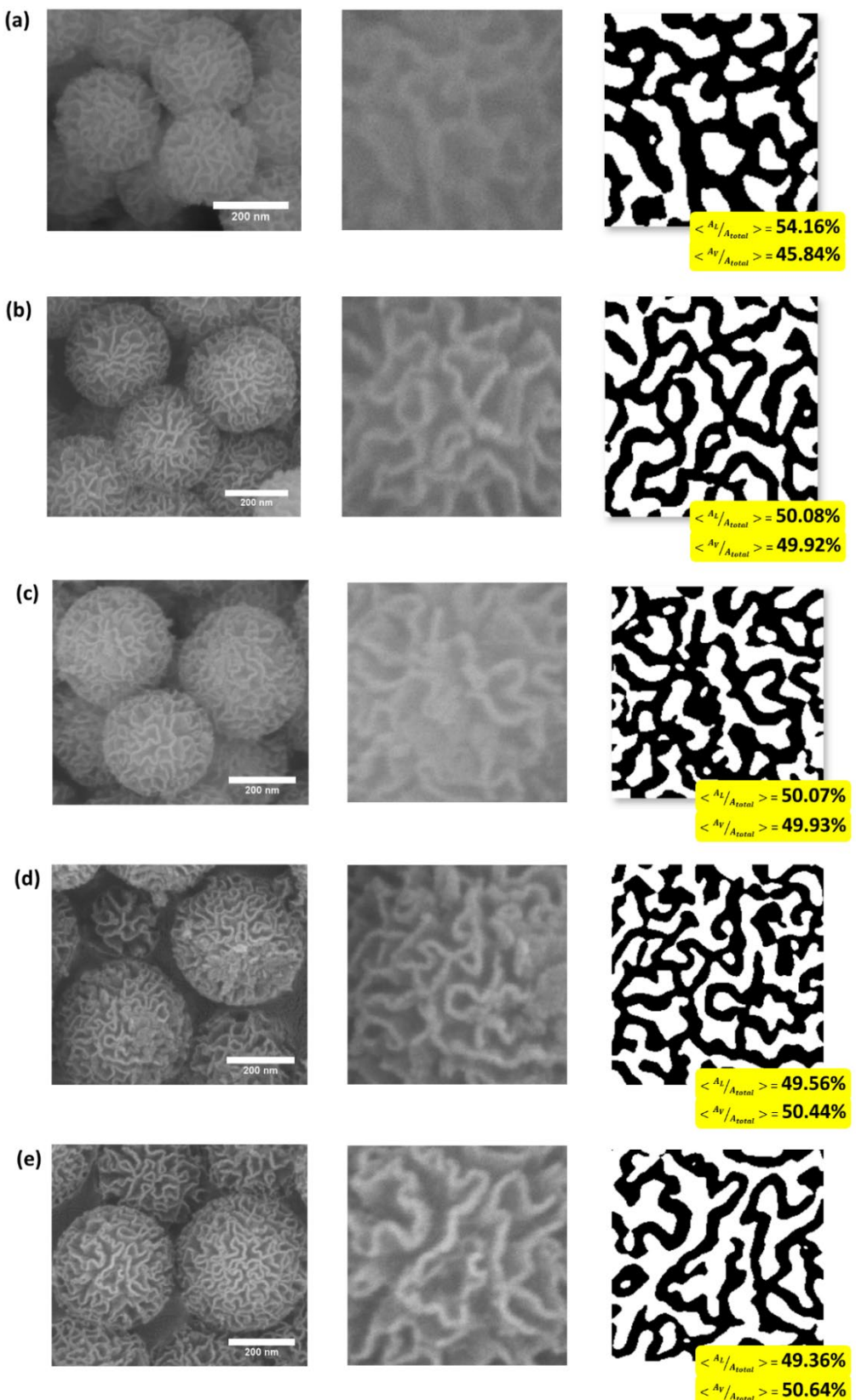
<sup>f</sup> Advanced Functional Materials (AFM) Laboratory, Department of Engineering Physics, Institut Teknologi Bandung, Bandung 40132, Indonesia.

<sup>g</sup> Center for Catalysis and Reaction Engineering, Institut Teknologi Bandung, Bandung 40132, Indonesia.

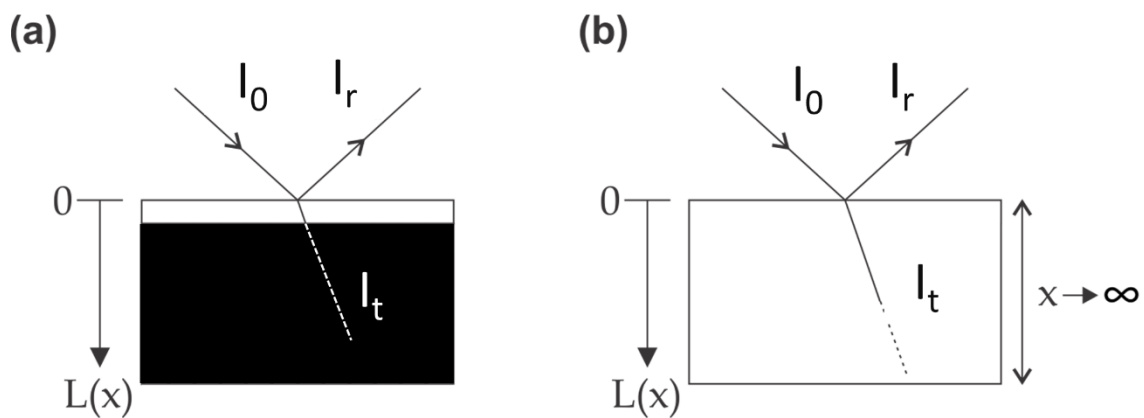
**\*Corresponding author:** vsuendo@itb.ac.id



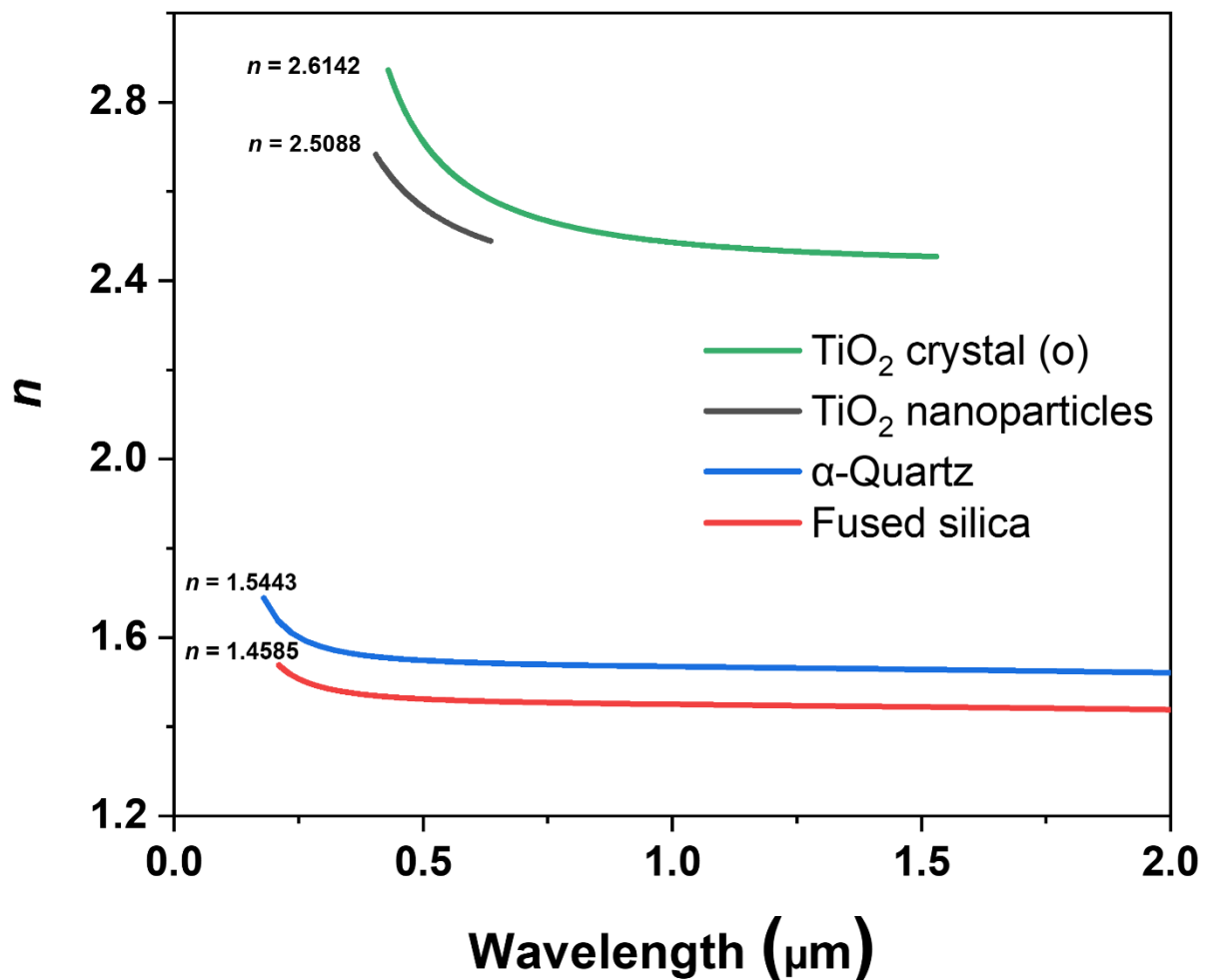
**Figure S1.** FESEM images and particle-size distributions of *bcl* silica that were synthesized at different times: (a) 6 h, (b) 8 h, (c) 12 h, (d) 18 h, and (e) 72 h.



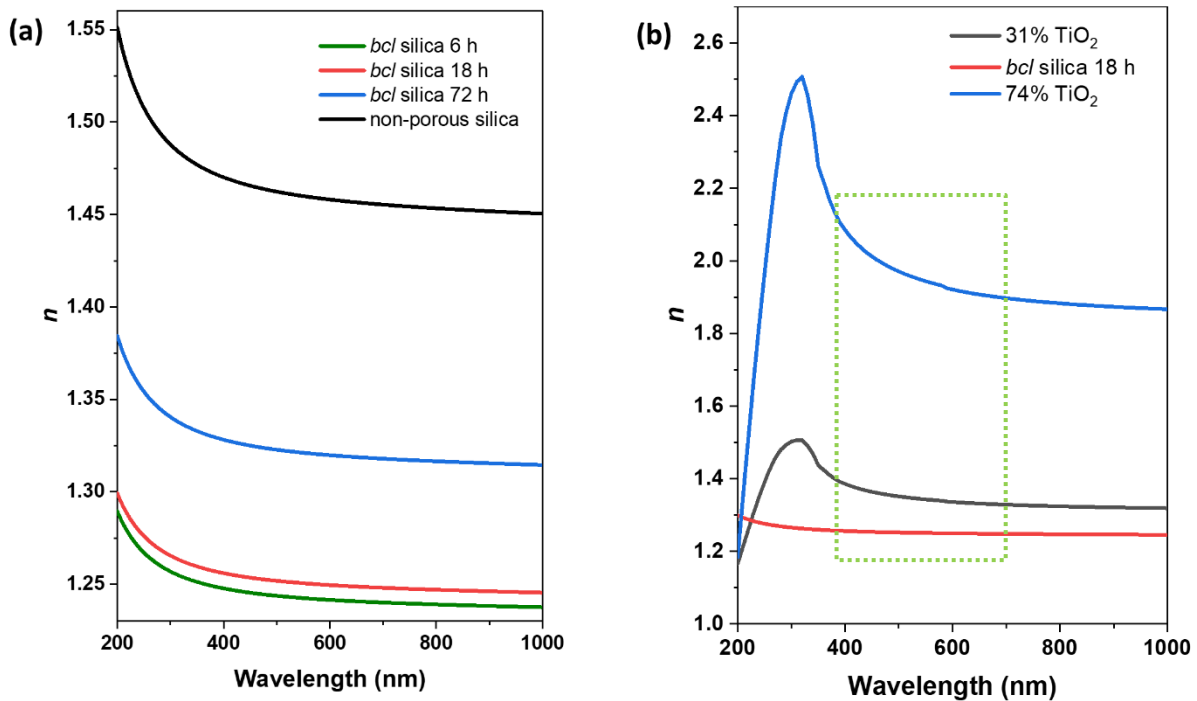
**Figure S2.** FESEM and binary images of *bcl* silica samples that were synthesized at different times: (a) 6 h, (b) 8 h, (c) 12 h, (d) 18 h, and (e) 72 h.



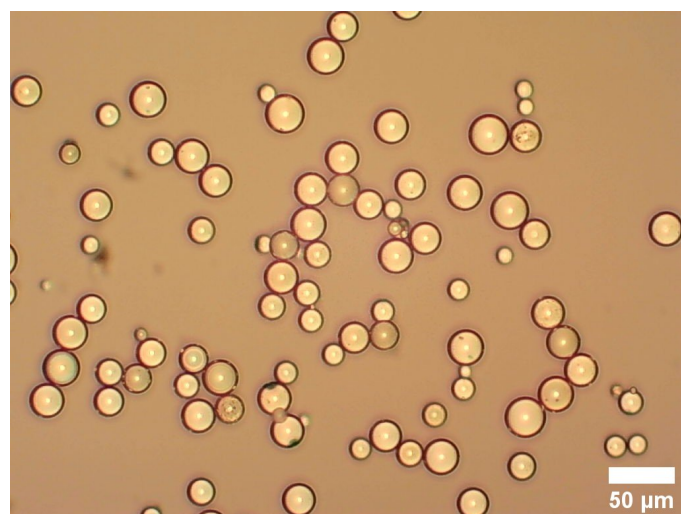
**Figure S3.** Kubelka-Munk model's light path. (a) The reflectance factor for a single sheet over a black background,  $R_0$  and (b) the reflectance when the specimen is infinitely thick,  $R_\infty$ .



**Figure S4.** Refractive index ( $n$ ) as a function of wavelength for TiO<sub>2</sub> crystals (ordinary ray),<sup>1</sup> TiO<sub>2</sub> nanoparticles,<sup>2</sup>  $\alpha$ -Quartz,<sup>3,4</sup> and fused silica.<sup>5,6</sup>



**Figure S5.** (a) The effective refractive index for *bcl* silica synthesized for different times compared with non-porous silica. (b) Comparison of the effective refractive indexes between the nano-spherical titania and *bcl* silica systems. The effective refractive index of nano-spherical titania film varied from the closed-packed system of hcp lattice with a filling factor of 0.74 (74%  $\text{TiO}_2$ ) to a 3D random contact network of packed spheres with the threshold of 0.31 (31%  $\text{TiO}_2$ ).<sup>7,8</sup> The green dotted line shows the visible light range. The effective refractive indexes are calculated using Bruggeman effective medium approximation by mixing the refractive index of pure silica/SiO<sub>2</sub><sup>9</sup> or titania/TiO<sub>2</sub> with the void in different volume fractions. The optical constants/refractive index of TiO<sub>2</sub> was obtained from the J.A. Woollam Co. materials database.

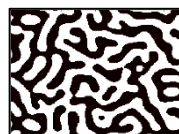


**Figure S6.** Microscope images of  $\text{SiO}_2$  microbeads.

**Table S1.** The quantization results of the Cahn-Hilliard spinodal decomposition model (variation in D values)

D	Gamma	Iterations	Simulation results	A <sub>L</sub> /A <sub>total</sub> (%)
5	5	10000		49.256
10	5	10000		49.654
15	5	10000		49.388
20	5	10000		49.654
25	5	10000		49.633

**Table S2.** The quantization results of the Cahn-Hilliard spinodal decomposition model (variation in gamma values)

D	Gamma	Iterations	Simulation results	A <sub>L</sub> /A <sub>total</sub> (%)
10	3	10000		49.170
10	6	10000		49.348
10	9	10000		50.251
10	12	10000		48.939
10	14	10000		49.591

**Table S3.** The quantization results of the Cahn-Hilliard spinodal decomposition model (variation in the number of iterations)

D	Gamma	Iterations	Simulation results	A <sub>L</sub> /A <sub>total</sub> (%)
10	3	10000		49.170
10	3	20000		49.594
10	3	30000		49.010
10	3	40000		49.832
10	3	50000		49.559
10	3	60000		49.331

**Table S4.** The average calculation of Shannon entropy of the FESEM image before thresholding

Synthesis time (h)	FESEM images before thresholding			Graph	$\langle H \rangle$
	1	2	3		
6					5.213
8					5.963
12					5.575
18					6.486
72					6.440

### Additional References:

- 1 J. R. DeVore, Refractive indices of rutile and sphalerite, *Journal of the Optical Society of Amerika*, 1951, **41**, 416–419.
- 2 I. Bodurov, I. Vlaeva, A. Viraneva, T. Yovcheva and S. Sainov, Modified design of a laser refractometer, *Nanoscience & Nanotechnology*, 2016, **16**, 31–33.
- 3 T. Radhakrishnan, in *Proceedings of the Indian Academy of Sciences-Section A*, Springer India, 1947, vol. 25, p. 260.
- 4 T. Radhakrishnan, in *Proceedings of the Indian Academy of Sciences-section A*, Springer India, 1951, vol. 33, p. 22.
- 5 I. H. Malitson, Interspecimen comparison of the refractive index of fused silica, *Journal of the Optical Society of Amerika*, 1965, **55**, 1205–1209.
- 6 C. Z. Tan, Determination of refractive index of silica glass for infrared wavelengths by IR spectroscopy, *Journal of Non-Crystalline Solids*, 1998, **223**, 158–163.
- 7 M. J. Powell, Site percolation in randomly packed spheres, *Phys. Rev. B*, 1979, **20**, 4194–4198.

- 8 R. M. Ziff and S. Torquato, Percolation of disordered jammed sphere packings, *J. Phys. A: Math. Theor.*, 2017, **50**, 085001.
- 9 E. D. Palik, *Handbook of Optical Constants of Solids*, Academic Press, 1st edn., 1991, vol. 2.